

Many-Body Effects on Nuclear Short Range Correlations

Haoyu Shang,¹ Jiawei Chen,¹ Rongzhe Hu,¹ Xin Zhen,¹ Chongji Jiang,¹ and J.C. Pei^{1,2,*}

¹State Key Laboratory of Nuclear Physics and Technology,
School of Physics, Peking University, Beijing 100871, China

²Southern Center for Nuclear-Science Theory (SCNT),
Institute of Modern Physics, Chinese Academy of Sciences, Huizhou 516000, China

We reveal nuclear many-body effects on short range correlations by *ab initio* no-core shell model calculations of the scaling factor a_2 . The factor a_2 characterizes the abundance of SRC pairs and is linearly related to the EMC effect. By calculating a_2 in light nuclei using the chiral N^4 LO nuclear force, including the ground state and excited states, and isobaric analog states in neighboring nuclei, we find that a_2 is close in isobaric analog states, while it varies in excited or isomeric states. This is explained as specific nuclear states suppress the formation of deuteron-like component, impacting elaborate understandings of SRC pairs in exotic nuclei.

Introduction.— Nuclear short-range correlations (SRC) exhibit an unique link across the energy scales from low to high energy nuclear physics [1]. It was revealed that high momentum nucleons in nuclei tend to form SRC pairs, with large relative momentum and smaller centre-of-mass (c.m.) momentum [2, 3]. The SRC pairs embody the realistic nucleon-nucleon interaction at short distances and have universal behaviors at high momentum in all nuclei [4–6]. On the other hand, it is of fundamental interests to understand the quark-gluon effects inside nuclei by analyzing SRC contributions to nuclear parton distribution functions [1, 2, 7, 8].

SRCs are usually characterized by the scaling factor $a_2(A/d)$, which measures the probability of finding a two-nucleon SRC pair in the nucleus relative to deuteron by inclusive high-energy electron scattering experiments [4, 8–11]. It can be calculated by evaluating the ratio of the high-momentum tail of the nucleon momentum distribution [2, 12, 13]. The scaling factor a_2 is linearly related to the magnitude of EMC effect [7]. Further exclusive measurements find that *np*-SRCs dominate whereas *pp*-SRCs have almost negligible contribution [14–17]. Currently, the probability of finding *np*-SRC pairs in a nucleus composed of Z protons and N neutrons is evaluated as $L\frac{NZ}{A}$, where L being the Lvinger constant [6, 18, 19]. In principle, the factor a_2 is expected to be dependent on specific nuclear structures, and this issue becomes essential to understand more precise measurements in the future.

The repulsive feature of *nn* and *pp* correlation functions at short ranges already appear [20], considering the influence of Pauli principle in the Fermi gas model or mean-field models, while *np* pairs are allowed at short ranges. To extract many-body effects on SRC beyond the mean field, *ab initio* calculations of the scaling factor a_2 with realistic nuclear forces are needed. Actually many-body wave functions in different nuclei can be factorized into a product of a universal short-range pair and a residual $A-2$ part [21]. To probe short-range structures, *ab initio* calculations require the use of hard nuclear interactions, which restrict the applicability of

many numerical methods. Variational Monte Carlo calculations (VMC) are able to handle hard interactions and give access to properties of a range of light nuclei [22–24]. However, VMC is restricted to local interactions [25, 26] and currently provide momentum distributions only for the ground state. Most chiral nucleon-nucleon (NN) interactions are developed in momentum space and are non-local [27–31]. In this respect, no-core shell model (NCSM) is an ideal full-configuration many-body method that can handle both local and non-local nuclear forces [32]. Furthermore, NCSM is a natural choice to distinguish many-body effects on SRC in nuclear states associated with different angular momentum, parity and isospin.

In this Letter, to study many-body effects on SRC, we develop NCSM calculations of a_2 in different states of ${}^6\text{Li}$. Specifically, we studied its ground state 1^+ , as well as the first and second excited states 3^+ and 0^+ . This is an appealing example to demonstrate many-body effects on SRC, as ${}^6\text{Li}$ has a core of ${}^4\text{He}$ plus a valence *np* pair. It is expected that the valence *np* pair in different configurations should have distinct contributions to SRC, in contrast to the tightly bound ${}^4\text{He}$ core. Moreover, the 0^+ state in ${}^6\text{Li}$, corresponding to ground states in ${}^6\text{He}$ and ${}^6\text{Be}$, are isobaric analog states. In this Letter, it is striking to find that the isobaric analog states in three nuclei have close a_2 values although their proton and neutron numbers are very different. In our NCSM calculations, the latest fifth-order (N^4 LO) nonlocal chiral interaction [28] are employed. To calculate a_2 , it is crucial to obtain translationally invariant (ti) one-nucleon momentum distributions [33], and this is realized by unfolding the c.m. motion from the one-nucleon density in the momentum space.

Translationally invariant density.— NCSM calculations conventionally adopt single-particle coordinates rather than relative coordinates. As a result, wave functions $\psi(\vec{k}_i)$ include c.m. motion and this is a key issue for calculating the scaling factor a_2 . The harmonic oscillator (HO) basis and full N_{max} truncation result in the exact factorization of the wave functions into a c.m. wave

function and a ti wave function [34]:

$$\psi^\omega(\vec{k}_1, \vec{k}_2, \dots, \vec{k}_A) = \phi_{\text{cm}}^\omega(\vec{K}) \psi_{\text{ti}}(\vec{k}_{\text{rel}1}, \vec{k}_{\text{rel}2}, \dots, \vec{k}_{\text{rel}A}), \quad (1)$$

where $\vec{K} = \sum_{i=1}^A \vec{k}_i$ and $\vec{k}_{\text{rel}} = \vec{k} - \frac{\vec{K}}{A}$. The c.m. wave function is $\phi_{\text{cm}}^\omega(\vec{K}) = e^{-K^2 \nu^2 / 2} (\frac{\nu}{\sqrt{\pi}})^{3/2}$, where $\nu = \frac{b}{\sqrt{A}}$ with $b = \sqrt{\frac{\hbar}{m\omega}}$ being the HO length.

The space-fixed (sf) density [35, 36] is obtained by the integral of $|\psi^\omega|^2$, which depends on the HO basis frequency ω . The ti density $\rho_{\text{ti}}(\vec{k})$ is obtained by integral of $|\psi_{\text{ti}}|^2$, which describes the probability of finding a nucleon with momentum \vec{k} relative to the c.m. of the entire nucleus and does not depend on ω . These two densities are related by:

$$\rho_{\text{sf}}^\omega(\vec{k}) = \int \rho_{\text{ti}}(\vec{k} - \vec{K}/A) \rho_{\text{cm}}^\omega(\vec{K}) d^3 K, \quad (2)$$

where $\rho_{\text{cm}}^\omega = \phi_{\text{cm}}^\omega{}^2(\vec{K})$, which smears out ρ_{ti} .

The ti density reflects the intrinsic properties of the nucleus and can be used to extract the scaling factor, which is obtained by unfolding the c.m. motion from the directly calculated sf density using standard Fourier methods:

$$\rho_{\text{ti}}(\vec{k}) = F \left[\frac{F^{-1} [\rho_{\text{sf}}^\omega(\vec{q})](\vec{r})}{(2\pi)^3 A^3 F^{-1} [\rho_{\text{cm}}^\omega(A\vec{K})](\vec{r})} \right](\vec{k}). \quad (3)$$

In calculations of ti densities, there could be oscillations at high momentum by using the Fourier transformations. To solve this issue, the sf densities from NCSM are first extrapolated with a smoothing exponent and transformed into $\tilde{\rho}_{\text{sf}}(r)$. Then oscillations are sufficiently suppressed for heavier nuclei such as ${}^6\text{Li}$. For very light nuclei, such as ${}^3\text{He}$, the oscillation still exist and a match to universal function is applied [13]. Finally the angle-averaged ti densities can be derived as,

$$\rho_{\text{ti}}(k) = 4\pi \int j_K(kr) \frac{\tilde{\rho}_{\text{sf}}(r)}{e^{-\frac{r^2}{4A^2\nu^2}}} r^2 dr. \quad (4)$$

Extraction of scaling factor a_2 .— Theoretical predictions for the scaling factors are proposed to be obtained by evaluating ratios of two-nucleon distributions in the limit of infinitely large relative momentum [12, 37, 38]:

$$a_2(A/d) = \lim_{k \rightarrow \infty} \frac{2 \rho_2(A, k)}{A \rho_2(d, k)}, \quad (5)$$

where the two-nucleon distribution is defined as $\rho_2(A, k) = \langle \psi | \sum_{i < j}^A \delta(k - k_{ij}) | \psi \rangle / (4\pi k^2)$ and is normalized to the number of nucleon pairs. In momentum space, for $k \rightarrow \infty$ there is a simple relation between the one-nucleon and the two-nucleon momentum distributions [6]:

$$\begin{aligned} \rho_{\text{ti},A}^p(k) &= 2\rho_2^{pp}(A, k) + \rho_2^{np}(A, k) \\ \rho_{\text{ti},A}^n(k) &= 2\rho_2^{nn}(A, k) + \rho_2^{np}(A, k). \end{aligned} \quad (6)$$

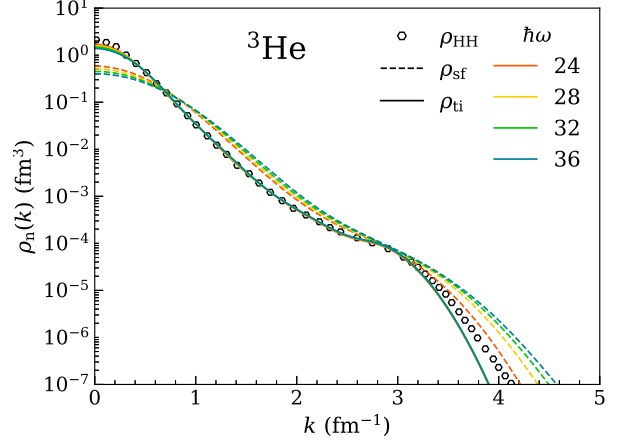


FIG. 1. Neutron momentum distribution of ${}^3\text{He}$ calculated by NCSM using the $N^4\text{LO}$ nonlocal NN interaction. The open circles represent results obtained by the HH method [39]. The dashed and solid lines correspond to the sf and ti densities, respectively, calculated by NCSM with $N_{\text{max}} = 16$, and $\hbar\omega$ ranging from 24 MeV to 36 MeV.

Consequently, the two-nucleon momentum distributions in Eq. (5) can be substituted by one-nucleon momentum distribution to evaluate the scaling factor:

$$a_2(A/d) = \lim_{k \rightarrow \infty} \frac{\rho_{\text{ti},A}(k)}{A |\tilde{\psi}_d(k)|^2} \approx \frac{\int_{k_0}^{\infty} \rho_{\text{ti},A}(k) k^2 dk}{A \int_{k_0}^{\infty} |\tilde{\psi}_d(k)|^2 k^2 dk}. \quad (7)$$

Here k_0 is typically chosen to be in the same range as fermi momentum ($k_F \approx 1.4 \text{ fm}^{-1}$). The integral of ti density is usually adopted for smooth estimations of a_2 [3, 12, 13].

Results and analysis.— Firstly we calculate the neutron density distribution of ${}^3\text{He}$ using NCSM with the bare $N^4\text{LO}$ nonlocal NN interaction EMN500 [28], to benchmark with the hyperspherical harmonics (HH) method [39], as shown in Fig.1. The NCSM code is taken from Ref. [40]. The sf densities are calculated at $N_{\text{max}} = 16$ with $\hbar\omega$ ranging from 24 MeV to 36 MeV. The chosen value of N_{max} is sufficient to get convergence in densities. The HH method, by employing Jacobi coordinates, avoids the c.m. problem [41]. Then ti densities from NCSM calculations are benchmarked with the HH results [39] to verify our procedure for unfolding the c.m. motion. Note that ti densities obtained using Eq. (4) exhibit small oscillations at high momentum larger than 3.8 fm^{-1} . To mitigate the oscillations, the matching ti densities after 2.0 fm^{-1} are shown. The difference in the high momentum range suggests that the high momentum part does not fully contribute from the low partial-wave universal functions. Additionally, the $\hbar\omega$ dependence of the sf densities is removed in the ti densities after unfolding the c.m. motion. It can be seen that the ti densities

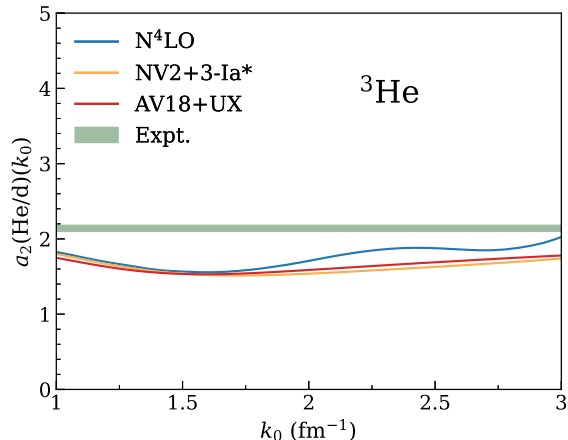


FIG. 2. The k_0 dependence in the estimation of the scaling factor a_2 for ${}^3\text{He}$ based on Eq.(7). For comparison, the results using densities from VMC calculations [22, 23] with AV18+UX and NV2+3-Ia potentials are also shown. The $N^4\text{LO}$ nonlocal NN interaction is adopted in NCSM calculations. The experimental value is indicated by the horizontal band.

match quite well with the HH results.

In Fig. 2, the k_0 dependence of the scaling factor a_2 are shown, as given by Eq.(7). The results are obtained using three different realistic NN nuclear forces: the local phenomenological force AV18 [26], the local Δ -full chiral force NV2 [25], and the nonlocal chiral force $N^4\text{LO}$ [28]. The AV18 and NV2 results are obtained by using densities from [22, 23], which includes three-body forces. It is shown that the ratios appear to be not sensitive to different nuclear interactions. As pointed out in Ref. [3], the high momentum dependence cancels out in the ratios. Furthermore, it can be observed that over a wide range of k_0 , the ratio of the integrated density remains relatively unchanged. We choose $k_0 = 2 \text{ fm}^{-1}$ to evaluate the scaling factor in the following, as suggested in Refs. [3, 12]. We also find that all estimations are slightly below the experimental data [8]. Such a discrepancy may indicate that k_0 in the numerator could be slightly smaller than that in the denominator of Eq. (7), considering their different minimum recoil momentum [42].

Next we extend the calculations to ${}^6\text{Li}$, for which no results with nonlocal chiral forces have been reported. In Fig. 3 we show the ti densities for two sets of finite basis spaces, with $\hbar\omega=28 \text{ MeV}$ and 36 MeV , respectively. The ti densities shown here are extracted directly using Eq. (4) without the matching procedure as there are no oscillations at high momentum, in contrast to ${}^3\text{He}$. Due to the limitation of computational resources, we are only able to reach a truncation at $N_{\text{max}} = 14$. As shown in Fig. 3, the high momentum tail converges more rapidly in a HO basis with $\hbar\omega = 36 \text{ MeV}$ than $\hbar\omega = 28 \text{ MeV}$. Therefore, in the following studies of $A = 6$ nuclei, we

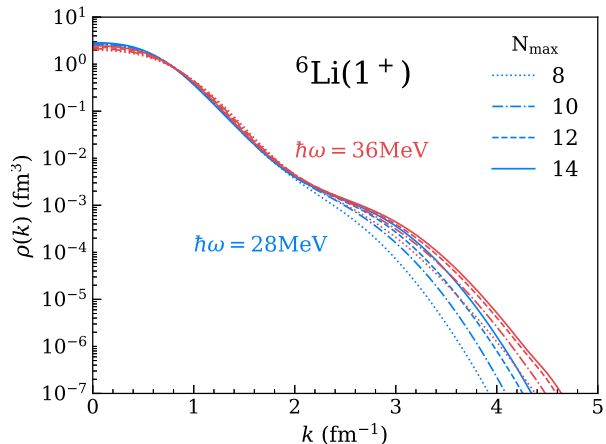


FIG. 3. The momentum distribution of the ground state of ${}^6\text{Li}(1^+)$, which are obtained by NCSM calculations with the $N^4\text{LO}$ nonlocal force for various N_{max} at $\hbar\omega = 28$ and 36 MeV , respectively.

adopt $\hbar\omega = 36 \text{ MeV}$ consistently. Note that $\hbar\omega = 36 \text{ MeV}$ is also the HO basis that minimizes the ground-state energy.

To demonstrate the many-body effects, the scaling factors of 1^+ ground state, as well as the subsequent 3^+ and 0^+ excited states are shown in Fig. 4, in which $\hbar\omega = 36 \text{ MeV}$ and $k_0 = 2 \text{ fm}^{-1}$ are adopted. The calculated excited energies of 3^+ and 0^+ are 2.68 and 4.19 MeV , respectively, which agree reasonably with experimental data 2.186 and 3.563 MeV . There is some k_0 dependence, which is similar to ${}^3\text{He}$, but the relative order of the scaling factors remains unchanged as k_0 varies. It is shown that a_2 becomes larger in 3^+ state but decreases significantly at 0^+ state. Usually we expect that less-bound excited states are more spatially spread out and should have reduced SRC. It has been pointed out that the EMC effect increases with increasing scaled nuclear densities [43]. Our results indicate that nuclear states with specific configurations, i.e. different angular momentum and parity, play a significant role in determining SRC pairs.

To further understand the influences of specific nuclear states, we consider the $T = 1$ ${}^6\text{He}$ - ${}^6\text{Li}$ - ${}^6\text{Be}$ isobaric triplet 0^+ states. Due to isospin symmetry, these 0^+ states are expected to have similar structures, which is supported by NCSM calculation showing that they exhibit close scaling factors. This implies that, in these isobaric analog states, certain np pairs in ${}^6\text{Li}$ have similar contributions to SRC as nn pairs in ${}^6\text{He}$ (or pp pairs in ${}^6\text{Be}$), leading to a suppression of SRC pairs. The scaling factor in ${}^4\text{He}$ is calculated to be 3.4 by NCSM. Then the estimated number of SRC pairs ($A \times a_2$) in ${}^4\text{He}$ is slightly smaller than that of the triplet 0^+ states. Note that for ground states in ${}^6\text{Li}$ and ${}^6\text{He}$, calculated a_2 with densities from VMC using AV18 agree well with our NCSM results.

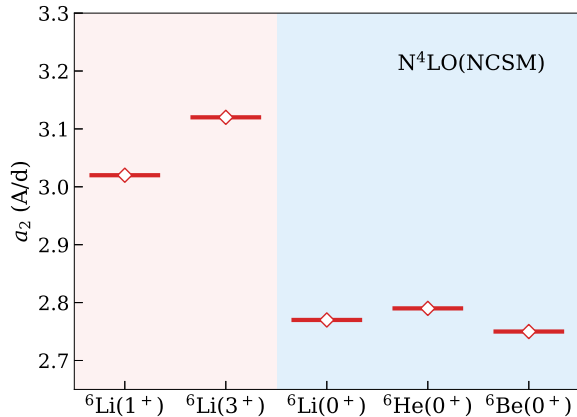


FIG. 4. The scaling factors a_2 of different nuclear states in ${}^6\text{Li}$ extracted with $k_0 = 2 \text{ fm}^{-1}$ using densities from NCSM calculations with $\hbar\omega = 36 \text{ MeV}$. Results of 0^+ ($T = 1$) isobaric triplet states in three neighboring nuclei are also displayed.

It is striking that 0^+ state in ${}^6\text{Li}$ has similar SRC pairs as ${}^6\text{He}$ and ${}^6\text{Be}$. To simplify the analysis of the formation of SRC pairs, we utilize an effective Hamiltonian to describe the $A=6$ system of two valence nucleons around a ${}^4\text{He}$ core, since the configuration mixing in NCSM framework are too complex. In this framework, the differences between the states arise solely from the configurations of the two valence nucleons. The shell model calculations are done within the $\pi(0p_{3/2}, 0p_{1/2}) \otimes \nu(0p_{3/2}, 0p_{1/2})$ model space using the ckpot [44] effective interaction. The configuration components are listed in Table I. The Moshinsky transformation [45, 46] is applied to extract the relative angular momentum between two valence nucleons from the single-particle configurations. The extracted possibilities of 3S_1 component are used as an indicator for the abundance of deuteron-like component. The 3S_1 components in 1^+ , 3^+ and 0^+ states in ${}^6\text{Li}$ are 36.63%, 50% and 0%, respectively, which follow the same order as the scaling factors a_2 . Therefore we can con-

TABLE I. The extracted probabilities of 3S_1 components in states of ${}^6\text{Li}$. The probabilities of 3S_1 is obtained by shell model calculations with two valence nucleons and the Moshinsky transformation. The configurations of two nucleons and the configuration components are listed in the 3rd and 4th column, respectively.

J^π	3S_1 (%)	Configurations	components (%)
1^+	36.63	$(\pi 0p_{3/2})^1 \otimes (\nu 0p_{3/2})^1$	36.82
		$(\pi 0p_{1/2})^1 \otimes (\nu 0p_{3/2})^1$	31.57
		$(\pi 0p_{3/2})^1 \otimes (\nu 0p_{1/2})^1$	31.57
3^+	50.00	$(\pi 0p_{3/2})^1 \otimes (\nu 0p_{3/2})^1$	100
0^+	0.00	$(\pi 0p_{3/2})^1 \otimes (\nu 0p_{3/2})^1$	76.00
		$(\pi 0p_{1/2})^1 \otimes (\nu 0p_{1/2})^1$	24.00

clude that the abundance of SRC pairs inside nuclei can be enhanced by the formation of deuteron-like component. However, np pairs can not form deuteron-like pairs in some specific quantum states. For example, 1S_0 ($T=1$) rather than 3S_1 is dominated in these 0^+ isobaric analog states, which has negligible contributions to SRC. In this case, SRC is not favored although valence protons and neutrons are in the same orbitals. This reveals that it is insufficient to estimate SRC pairs by only considering the neutron and proton numbers, and their mean-field shell structures.

Discussions.— Nuclear short-range correlations have broad implications in understandings of nuclear forces [15, 17], dense nuclear matter [47–49], modification of quark-gluon effects and EMC effects inside nuclei [7, 8, 50]. In this Letter, nuclear many-body effects in calculations of the scaling factor a_2 , which characterizes short-range correlations, have been demonstrated by *ab initio* no-core shell model calculations. The key step is to unfold the c.m. motion in densities in momentum space. The high precision $N^4\text{LO}$ chiral nucleon-nucleon force is adopted and the results of ${}^3\text{He}$ agree reasonably with experiments. To demonstrate the many-body effects, the scaling factors of the ground state and excited states of ${}^6\text{Li}$ are studied, which shows that the abundance of SRC pairs increases slightly in 3^+ state but decreases significantly in 0^+ state, compared to the ground state 1^+ . It is striking to find that a_2 is close in the 0^+ isobaric analog states in ${}^6\text{Li}$, ${}^6\text{Be}$, and ${}^6\text{He}$, although their neutron and proton numbers are different. This is explained as that the formation of deuteron-like components is suppressed in certain nuclear states by analyzing the shell model configurations. Our work highlights that the many-body effects play a significant role in the formation of SRC pairs inside nuclei. This will be useful to guide experiments on SRC in short-lived exotic nuclei or isomeric states, by using hadronic probes such as the hydrogen target [51].

We are grateful to useful discussions with F.R. Xu, P. Yin, D. Bai. This work was supported by the National Key R&D Program of China (Grant No.2023YFA1606403, 2023YFE0101500), the National Natural Science Foundation of China under Grants No.12475118, 12335007. We also acknowledge the funding support from the State Key Laboratory of Nuclear Physics and Technology, Peking University (No. NPT2023ZX01).

* peij@pku.edu.cn

- [1] A.W. Denniston, T. Ježo, A. Kusina, N. Derakhshanian, P. Duwentäster, O. Hen, C. Keppel, M. Klasen, K. Kovářik et al. Phys. Rev. Lett. 133, 152502 (2024).
- [2] O. Hen, G. A. Miller, E. Piasetzky, and L. B. Weinstein, Rev. Mod. Phys. 89, 045002 (2017).

- [3] A. Tropiano, S. Bogner, and R. Furnstahl, *Phys. Rev. C* 104, 034311 (2021).
- [4] L. Frankfurt, M. Strikman, D. Day, and M. Sargsyan, *Phys. Rev. C* 48, 2451 (1993).
- [5] C. C. degli Atti, *Phys. Rep.* 590, 1 (2015).
- [6] R. Weiss, B. Bazak, and N. Barnea, *Phys. Rev. C* 92, 054311 (2015).
- [7] L.B. Weinstein, E. Piasetzky, D. Higinbotham, J. Gomez, O. Hen, and R. Shneor, *Phys. Rev. Lett.* 106, 052301 (2011).
- [8] B. Schmookler, D. S. Armbruster, T. C. Hsu, and S. P. Roberts, *Nature*, 566, 354 (2019).
- [9] K. S. Egiyan, N. Dashyan, M. Sargsian, M. Strikman, L. Weinstein, G. Adams, P. Ambrozewicz, M. Anghinolfi, B. Asavapibhop, G. Asryan, and C. Benesh, *Phys. Rev. Lett.* 96, 082501 (2006).
- [10] N. Fomin, J. Arrington, R. Asaturyan, F. Benmokhtar, W. Boeglin, P. Bosted, A. Bruell, M. Bukhari, M. Christy, E. Chudakov, and J. Watson, *Phys. Rev. Lett.* 108, 092502 (2012).
- [11] S. Li, R. Cruz-Torres, N. Santiesteban, Z. Ye, D. Abrams, S. Alsalmi, D. Androic, K. Aniol, J. Arrington, and T. Averett, *Nature*, 609, 41 (2022).
- [12] J. Ryckebusch, W. Cosyn, T. Vieijra, and C. Casert, *Phys. Rev. C* 100, 054620 (2019).
- [13] R. Weiss, R. Cruz-Torres, N. Barnea, E. Piasetzky, and O. Hen, *Phys. Lett. B* 780, 211 (2018).
- [14] R. Shneor, P. Monaghan, R. Subedi, B. Anderson, K. Aniol, J. Annand, J. Arrington, H. Benaoum, F. Benmokhtar, P. Bertin, and C. Carlson, *Phys. Rev. Lett.* 99, 072501 (2007).
- [15] I. Korover, N. Muangma, O. Hen, R. Shneor, V. Sulkosky, A. Kelleher, S. Gilad, D. Higinbotham, E. Piasetzky, J. Watson, and N. Wiesner, *Phys. Rev. Lett.* 113, 022501 (2014).
- [16] M. Duer, A. Schmidt, J. Pybus, E. Segarra, A. Hrnjic, A. Denniston, R. Weiss, O. Hen, E. Piasetzky, L. Weinstein, and R. Wiringa, *Phys. Rev. Lett.* 122, 172502 (2019).
- [17] A. Schmidt, J. Pybus, R. Weiss, E. Segarra, A. Hrnjic, A. Denniston, O. Hen, E. Piasetzky, L. Weinstein, N. Barnea, and R. Wiringa, *Nature*, 578, 540 (2020).
- [18] J. Levinger, *Phys. Rev.* 84, 43 (1951).
- [19] R. Weiss, B. Bazak, and N. Barnea, *Phys. Rev. Lett.* 114, 012501 (2015).
- [20] R. Cruz-Torres, A. Schmidt, G. A. Miller, L. B. Weinstein, N. Barnea, R. Weiss, E. Piasetzky, O. Hen, *Phys. Lett. B* 785, 304(2018).
- [21] R. Cruz-Torres, D. Lonardonì, R. Weiss, M. Piarulli, N. Barnea, D. Higinbotham, E. Piasetzky, A. Schmidt, L. Weinstein, and R. Wiringa, *Nat. Phys.* 17, 306 (2021).
- [22] R. B. Wiringa, R. Schiavilla, S. C. Pieper, and J. Carlson, *Phys. Rev. C* 89, 024305 (2014).
- [23] M. Piarulli, S. Pastore, R. Wiringa, S. Brusilow, and R. Lim, *Phys. Rev. C* 107, 014314 (2023).
- [24] J. Carlson, S. Gandolfi, F. Pederiva, S. C. Pieper, R. Schiavilla, K. E. Schmidt, and R. B. Wiringa, *Rev. Mod. Phys.* 87, 1067 (2015).
- [25] M. Piarulli, L. Girlanda, R. Schiavilla, A. Kievsky, A. Lovato, L. E. Marcucci, S. C. Pieper, M. Viviani, and R. B. Wiringa, *Phys. Rev. C* 94, 054007 (2016).
- [26] R. B. Wiringa, V. Stoks, and R. Schiavilla, *Phys. Rev. C* 51, 38 (1995).
- [27] D. Entem and R. Machleidt, *Phys. Rev. C* 68, 041001 (2003).
- [28] D. Entem, R. Machleidt, and Y. Nosyk, *Phys. Rev. C* 96, 024004 (2017).
- [29] A. Ekström, G. Baardsen, C. Forssén, G. Hagen, M. Hjorth-Jensen, G. Jansen, R. Machleidt, W. Nazarewicz, T. Papenbrock, J. Sarich et al., *Phys. Rev. Lett.* 110, 192502 (2013).
- [30] E. Epelbaum, W. Glöckle, and U.-G. Meißner, *Nucl. Phys. A* 747, 362 (2005).
- [31] P. Reinert, H. Krebs, and E. Epelbaum, *Eur. Phys. J. A* 54, 1 (2018).
- [32] B. R. Barrett, P. Navrátil, and J. P. Vary, *Prog. Part. Nucl. Phys.* 69, 131 (2013).
- [33] P. Navrátil, *Phys. Rev. C* 70, 014317 (2004).
- [34] D. Gloeckner and R. Lawson, *Phys. Lett. B* 53, 313 (1974).
- [35] C. Cockrell, J. P. Vary, and P. Maris, *Phys. Rev. C* 86, 034325 (2012).
- [36] B. Giraud, *Phys. Rev. C* 77, 014311 (2008).
- [37] J.-W. Chen, W. Detmold, J. E. Lynn, and A. Schwenk, *Phys. Rev. Lett.* 119, 262502 (2017).
- [38] J. Lynn, D. Lonardonì, J. Carlson, J. Chen, W. Detmold, S. Gandolfi, and A. Schwenk, *J Phys. G Nucl. Part. Phys.* 47, 045109 (2020).
- [39] L. E. Marcucci, F. Sammarruca, M. Viviani, and R. Machleidt, *Phys. Rev. C* 99, 034003 (2019).
- [40] N. Michel and M. Płoszajczak, *Gamow Shell Model*, 983, Springer (2021).
- [41] L. E. Marcucci, J. Dohet-Eraly, L. Girlanda, A. Gnech, A. Kievsky, and M. Viviani, *Front. Phys.* 8, 69 (2020).
- [42] K. Sh. Egiyan, N. Dashyan, M. Sargsian, et al., *Phys. Rev. C* 68, 014313(2003).
- [43] J. Seely, A. Daniel, D. Gaskell, et al., *Phys. Rev. Lett.* 103, 202301 (2009).
- [44] S. Cohen and D. Kurath, *Nucl. Phys.* 73, 1 (1965).
- [45] M. Moshinsky, *Nucl. Phys.* 13, 104 (1959).
- [46] B. Buck and A. Merchant, *Nucl. Phys. A* 600, 387 (1996).
- [47] L. Frankfurt, M. Sargsian, and M. Strikman, *Int. J. Mod. Phys. A*, 23, 2991 (2008).
- [48] O. Hen, B.-A. Li, W.-J. Guo, L. Weinstein, and E. Piasetzky, *Phys. Rev. C* 91, 025803 (2015).
- [49] B.-A. Li, B.-J. Cai, L.-W. Chen, and J. Xu, *Prog. Part. Nucl. Phys.* 99, 29 (2018).
- [50] E. P. Segarra, A. Schmidt, T. Kutz, D. Higinbotham, E. Piasetzky, M. Strikman, L. Weinstein, and O. Hen, *Phys. Rev. Lett.* 124, 092002 (2020).
- [51] M. Patsyuk, J. Kahlbow, G. Laskaris, et al. *Nat. Phys.* 17, 693 (2021).